Supporting Information

Revealing the carbohydrate pattern on the cell surface by super-resolution imaging

Junling Chen,[a b] *Jing Gao*,[a,b] *Jiazhen Wu*[a,b], *Min Zhang*[a,b], *Mingjun Cai*,[a] *Haijiao Xu*,[a] *Junguang Jiang*,[a] *Zhiyuan Tian*,[c] and *Hongda Wang* *[a]

[a] State Key Laboratory of Electroanalytical Chemistry, Changchun Institute of Applied Chemistry, Chinese Academy of Sciences, Changchun, Jilin 130022, P.R. China.

[b] University of Chinese Academy of Sciences, Beijing 100049, P.R. China.

[c] School of Chemistry and Chemical Engineering, University of Chinese Academy of Sciences, Beijing 100049, China

KEYWORDS: super-resolution imaging • carbohydrate • N-GlcNAc • cluster

1. The schematic diagram demonstrating how to image the apical and basal membranes with TIRF illumination.

In our research, we respectively imaged the apical and basal membranes with TIFR illumination at the same irradiation intensity. Before imaging, the small cover slide (22x22 nm) where cells were seeded was sealed on the large microscope slide (24x50 nm) with nail polish (Figure S3A-left). When imaging the apical membrane , the large microscope slide was attached to the objective to facilitate focusing on the apical membrane by TIFR illumination (Figure S3A-middle); for the basal membrane, we put the small cover slide approach to the objective to make the basal membranes were the objective-proximal portion and easily imaged with TIRF illumination (Figure S3-right). The cross section (Figure S1B) can further demonstrate the detailed imaging conditions.

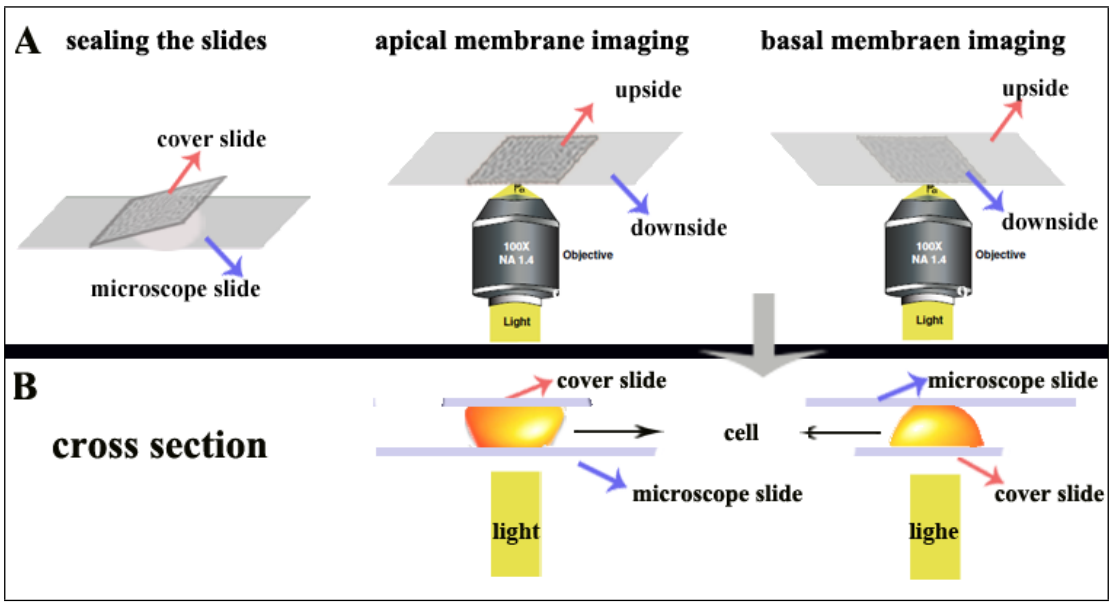

Figure S1. The schematic diagram of imaging the apical and basal membranes with TIRF illumination. (A) the schematic diagram demonstrating how to seal the slides (A-left), how to image the apical membranes (A-middle) and the basal membranes (A-right). (B). the corresponding cross section of imaging the apical and basal membranes.

2. Determining the average localization precision by measuring the single Alexa647-linked WGA on the clean glass slide

The WGA conjugated with Alexa647 were sparsely incubated on the clean glass slide at very low concentration (~0.2 nM) and mixed with Bovine Serum Albumin (BSA, Sigma). Then, it was imaged under the same imaging condition as the experimental sample (Figure.S1A). Because of the repeating localizations of single organic fluorophore, the localization precision can be calculated as the standard deviation of many fitted positions of the same molecule (Figure S2B). Therefore, we aligned 45 single WGA clusters by their mass center to achieve a 3D Gaussian profile (Figure S2C) and the 2D histogram of the localizations (Figure S2D). Through fitting the histogram to the Gaussian function, we obtained a full width at half maximum (FWHM) of 23.7±1.8 nm, indicating that the localization precise was ~24 nm for the conventional fluorescent probe on the glass slide. (Figure S2).

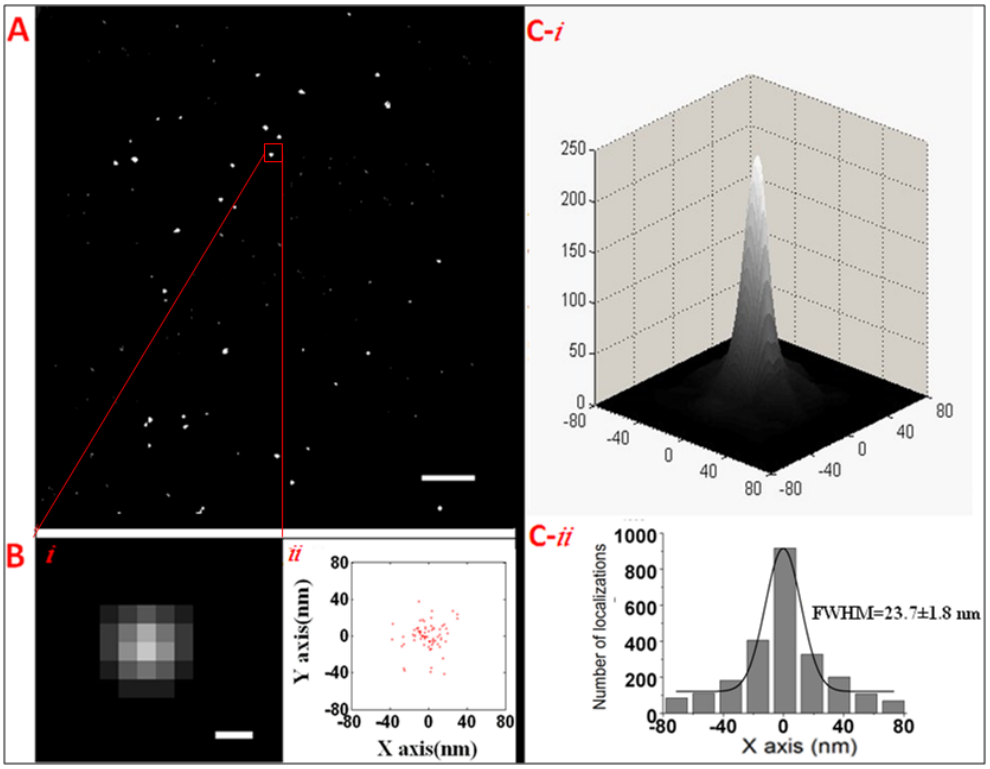

Figure S2. The localization precision of dSTORM imaging was determined by localizing single Alexa647-linked WGA. (A) dSTORM image of single Alexa647-linked WGAs which were sparsely distributed on a clean slide and separated by BSA. Scale bar, 2 μm. (B) The enlarged image of the boxed region in Figure A, showing the image of a single WGA. The corresponding repeating localizations between fluorescent and dark state were represented as crosses. Scale bar, 100 nm. The three-dimensional Gaussian profile (C) and two-dimensional histogram of localizations (D) generated by aligning 45 single WGA clusters by their center of

mass. The FWHM determined by Gaussian fitting demonstrates a localization precision is 23.7 ± 1.8 nm for conventional fluorescent probes.

3. Determining the localization precision of the single fluorescent probe on the cell surface

The localization precision on the cell surface was also determined by measuring the single Alexa647-linked WGA on the Vero basal membrane with the same method for the single Alexa647-WGA on glass slide. We found that the localization precision on the cell surface was 25.0±2.7 nm (Figure S3), which was close to data in Figure S2.

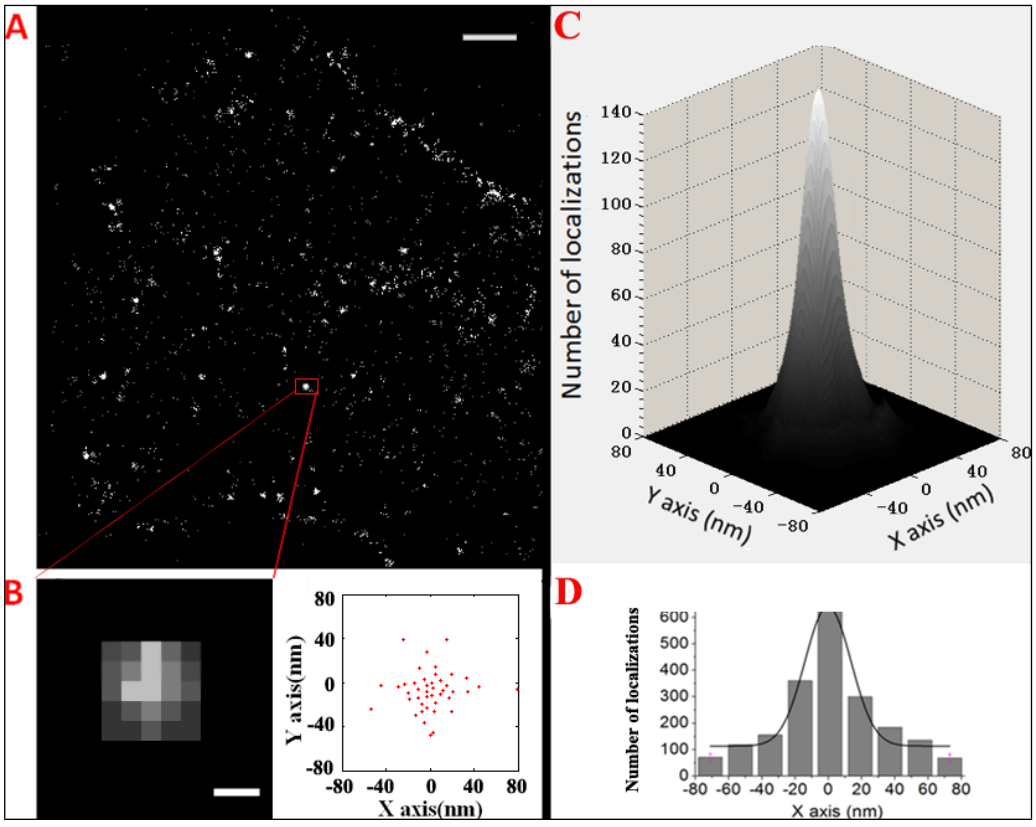

Figure S3. The localization precision of dSTORM imaging on the cell surface was determined by localizing single Alexa647-linked WGA on the Vero basal membrane. (A) dSTORM image of N-GlcNAcs on the Vero basal membranes at the low labeling concentrations (0.01 μM). Scale bar, 2 μm. (B) The localizations of single WGA as the Figure S1B. Scale bar, 100 nm. (C) the three-dimensional Gaussian profile (C) and the two-dimensional histogram of the localizations from many single WGA cluster generated by aligning 40 single WGA clusters by their center of mass. Then it was fitted to a Gaussian profile to determine the FWHM, demonstrating a localization precision of 25.0±2.7 nm on the cell surface.

4. Optimizing the labeling concentration of WGA on the Vero basal membranes by the concentration plot

We mapped N-GlcNAcs on the Vero basal membranes at different labeling concentrations of WGA, and calculated the density of localizations in the unit area of cell membranes. The statistic data of ten cells at each concentration were plotted to determine the saturated concentration, and it was ~0.1 μM (Figure S4).

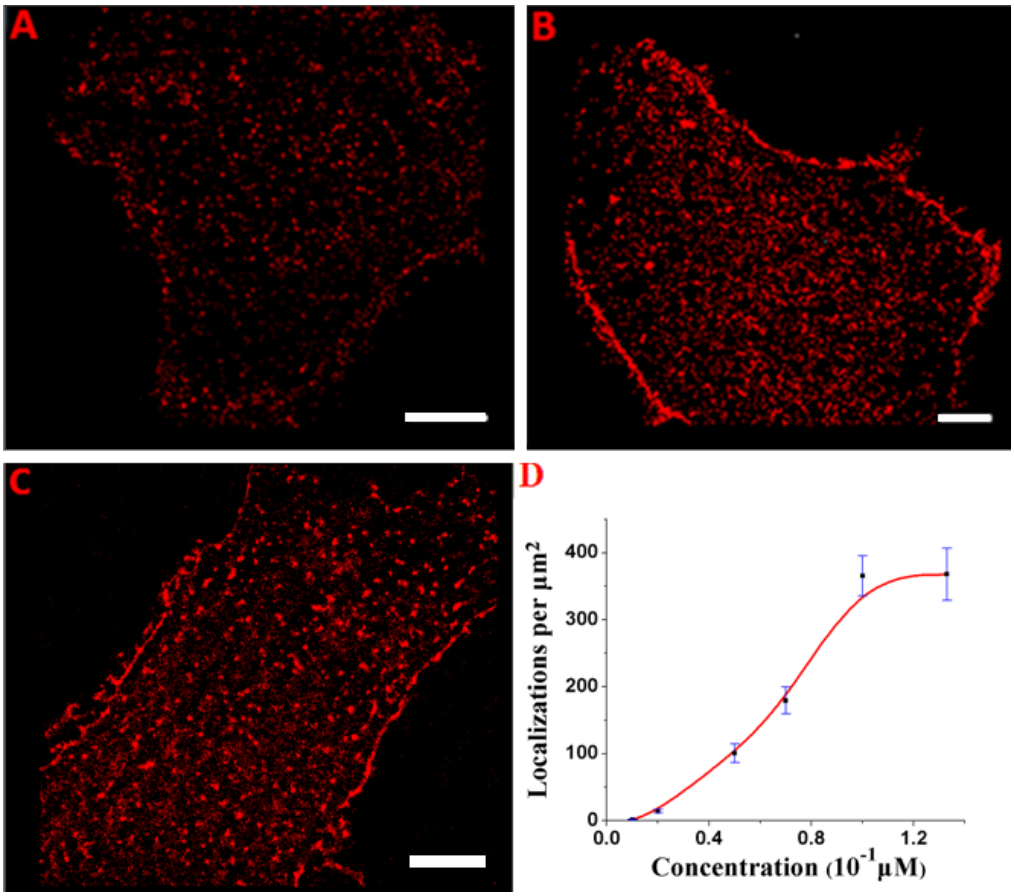

Figure S4. The saturated labeling concentration of Alexa647-linked WGA for basal membranes was determined by analyzing the density of localizations on dSTORM images while increasing labeling concentrations. (A–C) The dSTORM reconstruction images with increasing labeling concentrations, 0.02 μM (A), 0.05 μM (B) and 0.10 μM (C), respectively. (D) The plot of density (localizations per μm^2) at six labeling concentrations (0.1×, 0.2×, 0.5×, 0.7×, 1.0×, 1.3×10^{-1} μM), demonstrating that the saturated concentration is ~0.10 μM. The data were obtained from ten cells at each concentration. Scale bars are 5 μm in A–C.

5. Optimizing the labeling concentration of WGA on the Vero apical surface by the concentration plot

With the same method as optimizing the labeling concentration on the basal membrane (above), we obtained that the saturated labeling concentration of WGA for the apical membrane was ~0.08 μM (Figure S5).

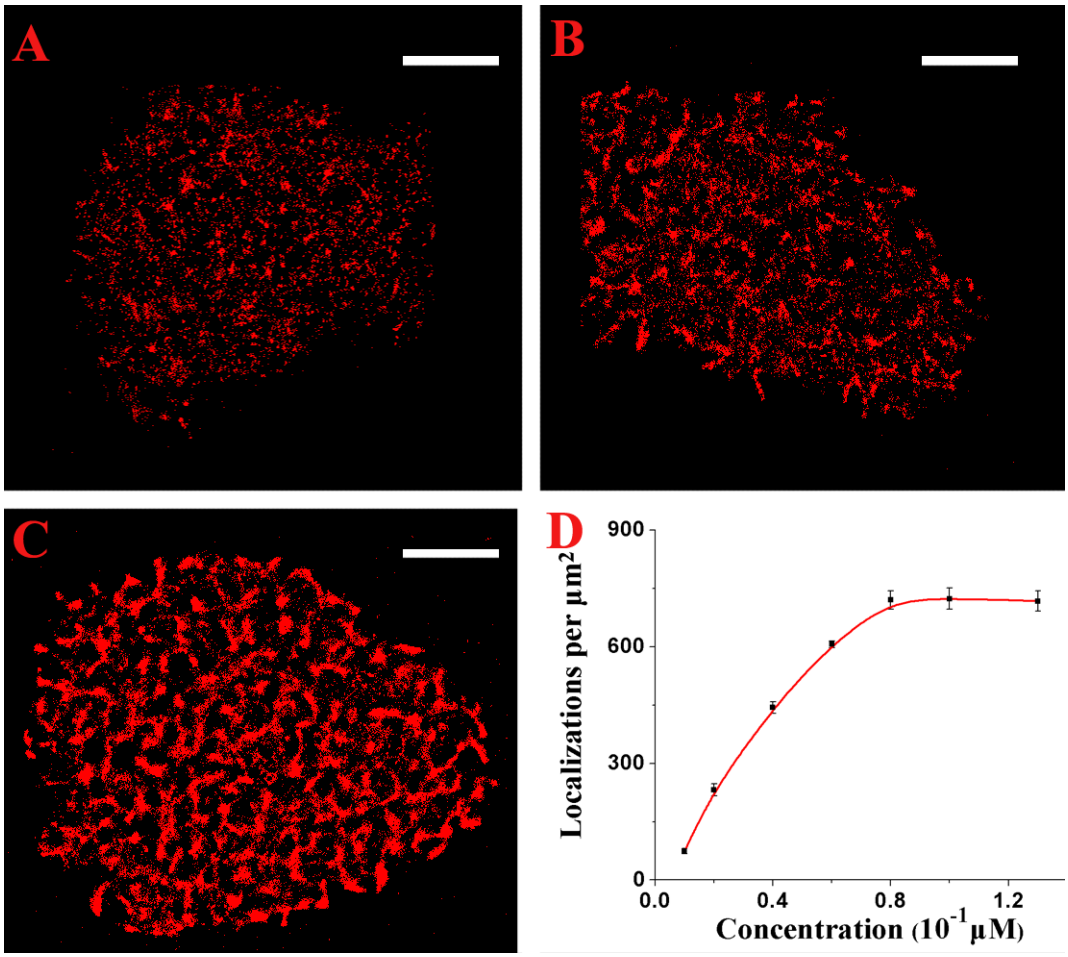

Figure S5. The saturated labeling concentration of Alexa647-linked WGA for the apical membrane was determined by the same method as the basal membrane. (A–C) The dSTORM images with increasing labeling concentrations, 0.02 μM (A), 0.06 μM (B) and 0.10 μM (C), respectively. (D) The plot of density (localizations per μm^2) at seven labeling concentrations (0.1×, 0.2×,0.4×, 0.6×, 0.8×, 1.0×, 1.3×10^{-1} μM), indicating that the saturated concentration is ~0.08 μM. The data were obtained from ten cells at each concentration. Scale bars are 5 μm in A–C.

6. The marked difference in the organization of N-GlcNAcs between on live cells and on fixed cells with different fixing time.

In our research, we implemented a series of the fixation experiments of 4% PFA with different fixing time. We found that the inadequate fixation (20 min) (Fig.S6A) could not effectively make the plasma membrane molecules immobile, leading to the molecules were affected by the induction of WGA to form the longer and larger clusters than those on the cells fixed with adequate time (40 or 50 min, Figure S6B and C). Additionally, according to the similar results between the fixation of 40 min and the fixation of 50 min (Figure S6B and C), we found that the fixation of 4% PFA with 40 min was a suitable and reasonable protocol in our experiment to effectively fix cells to get rid of the influence from WGA. Meanwhile, we imaged the organization of N-GlcNAcs on live cells (Figure S6D) and found it markedly differed from that on the adequately fixed cells (Figure S6B and C), and to some extent, was similar like that on the inadequately fixed cells (Figure S6A), indicating that the changed distribution pattern of N-GlcNAcs was likely caused by the agglutination of WGA. Compared with these different imaging results of different treatments, we can infer that fixing cell with sufficient time can effectively avoid the induced clustering by WGA. Moreover, we imaged the distribution of N-GlcNAcs on the Vero apical membrane fixed with 4% paraformaldehyde (PFA) and 0.2% glutaraldehyde (GA) (Figure S6E), and found it was similar as that with 4% PFA.

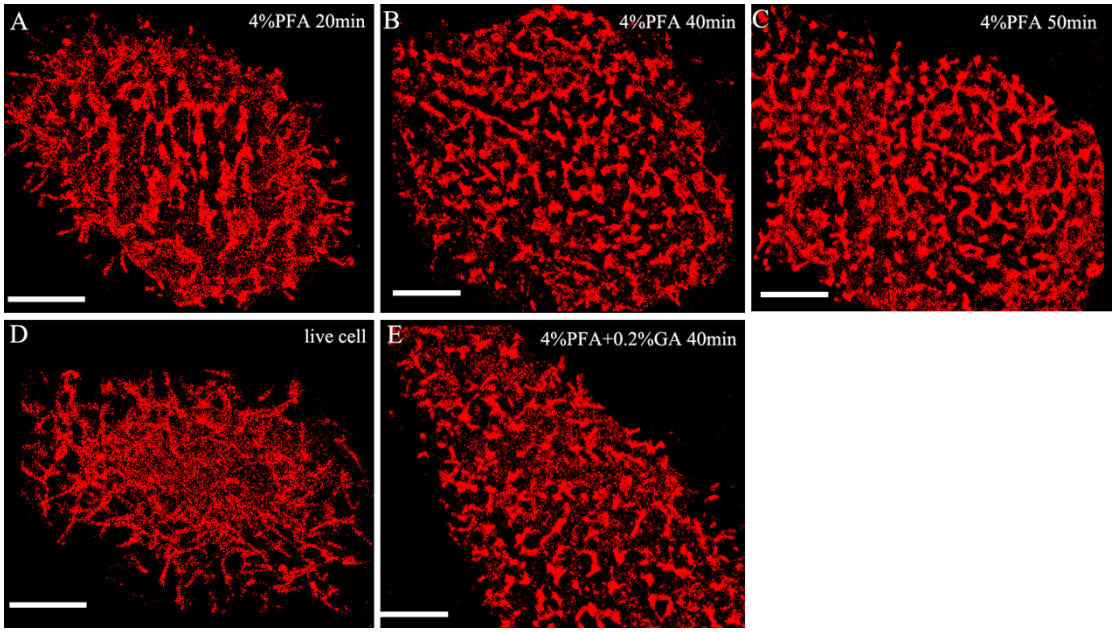

Figure S6. The super-resolution images of the distribution of N-GlcNAcs on the Vero apical membrane with different fixation treatments. The dSTORM imaging of N-GlcNAcs on the fixed apical membrane by 4% PFA with 20 min (A), 40 min (B) and 50 min (C). (D) the dSTORM imaging of N-GlcNAcs on the live cellular apical membrane. (E) the dSTORM imaging of N-GlcNAcs on the fixed cellular apical membrane by 4% PFA and 0.2% GA.

7. The 3D-deconvolution fluorescent imaging of N-GlcNAcs on the Vero cell membrane.

To make sure the N-GlcNAcs we imaged were the plasma membrane carbohydrates, we preformed the 3D-deconvolution fluorescent imaging of N-GlcNAcs and found no fluorescent molecule in the cellular interior with fixation of 40 min.

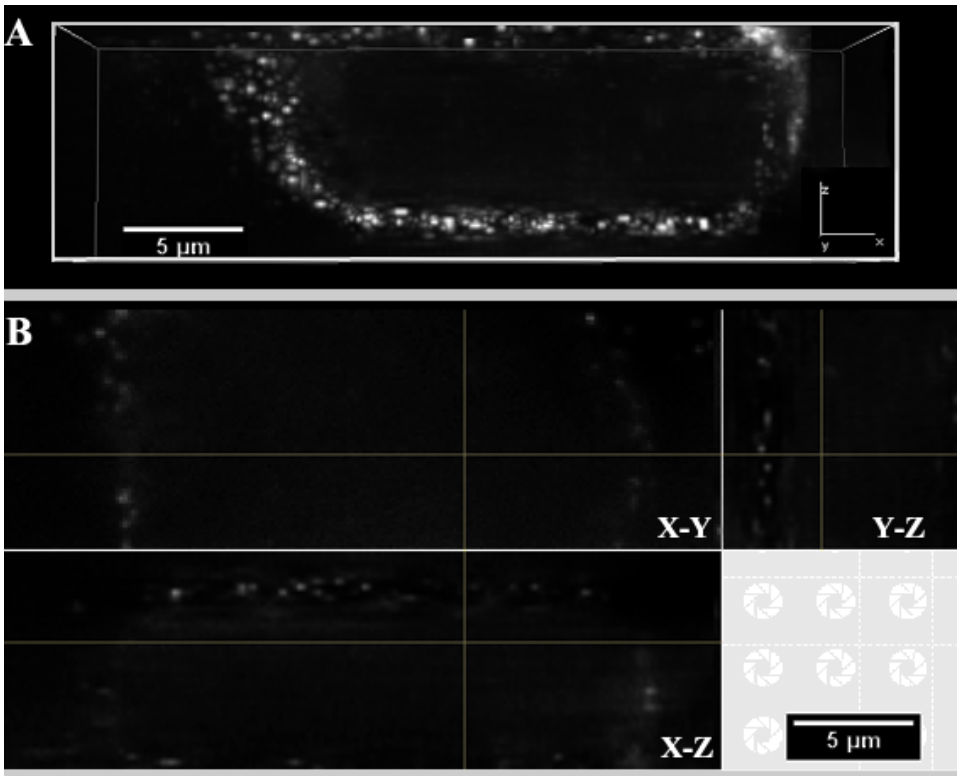

Figure S7. (A) The 3D-deconvolution fluorescent image of N-GlcNAcs on the Vero cell membrane. (B) the corresponding cross section images of N-GlcNAcs on the Vero cell membrane.

8. The non-specific labeling was ruled out by blocking experiment of 3% BSA

In order to examine the possibility of the non-specific binding in the experiments, we imaged N-GlcNAcs on the Vero apical surface blocked by 3% BSA that can effectively reduce the number of the non-specific bind sites[1], and found the results were very similar as those without the blocking of BSA, ruling out the possibility of the non-specific labeling during imaging (Figure S8).

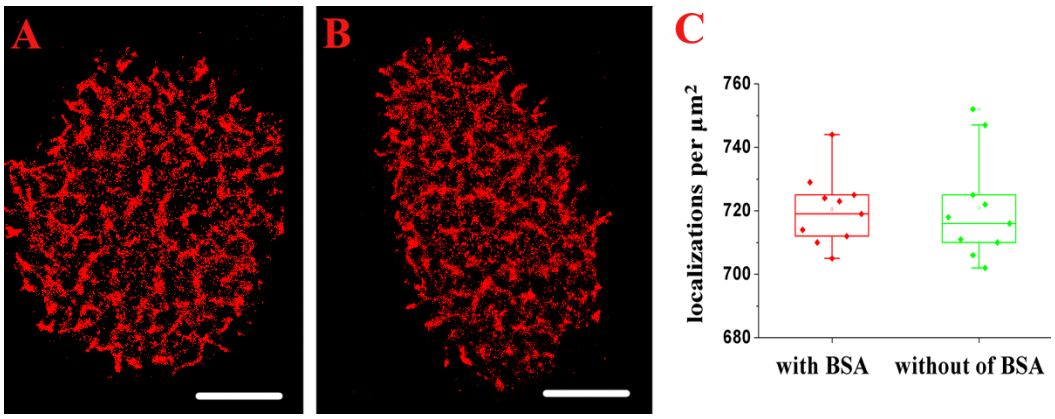

Figure S8. The dSTORM images of N-GlcNAcs on Vero apical membranes with (A) and without 3% BSA blocking (B). (C) The densities of localizations per unit area of cell membranes with and without 3% BSA, data from ten cells of three parallel experiments. Scale bars are 5 μm in A and B.

9. The procedure of the cluster analysis.

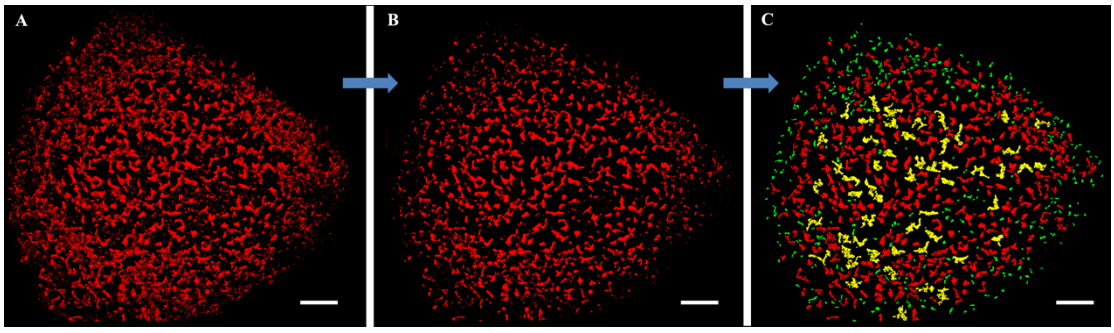

Figure S9. (A) The dSTORM image of N-GlcNAcs on the Vero apical membrane. (B) The image of N-GlcNAcs treated with the function of *denoise* in ImageJ to remove the sparse single points. (C) The image of the distribution of qualified clusters. Scale bars are 5 μm in A, B and C.

10. The frame number was determined by analyzing the distribution pattern of N-GlcNAcs in different images reconstructed from the increasing frame sequences

In our study, we paid more attention to the distribution pattern of N-GlcNAcs, so we determined the suitable flame number by analyzing the changes of the distribution pattern of N-GlcNAc with the increasing frame sequences. From Figure S10A, when the frame number was fewer than 5000, the appearance of cluster was not completely shown in the dSTORM images, and it changed a lot with increasing the frame

number. However, after 5000 frames, the cluster size was almost not enlarged, and the distribution pattern has a similar feature as that from 5000 frames, which is apparently demonstrated by the change of the individual enlarged cluster with increasing the frame number (Figure S10B). By statistically analyzing the trend of the average cluster size with increasing frame number (Figure S10C), we chose the first 5000 frames to reconstruct dSTORM image.

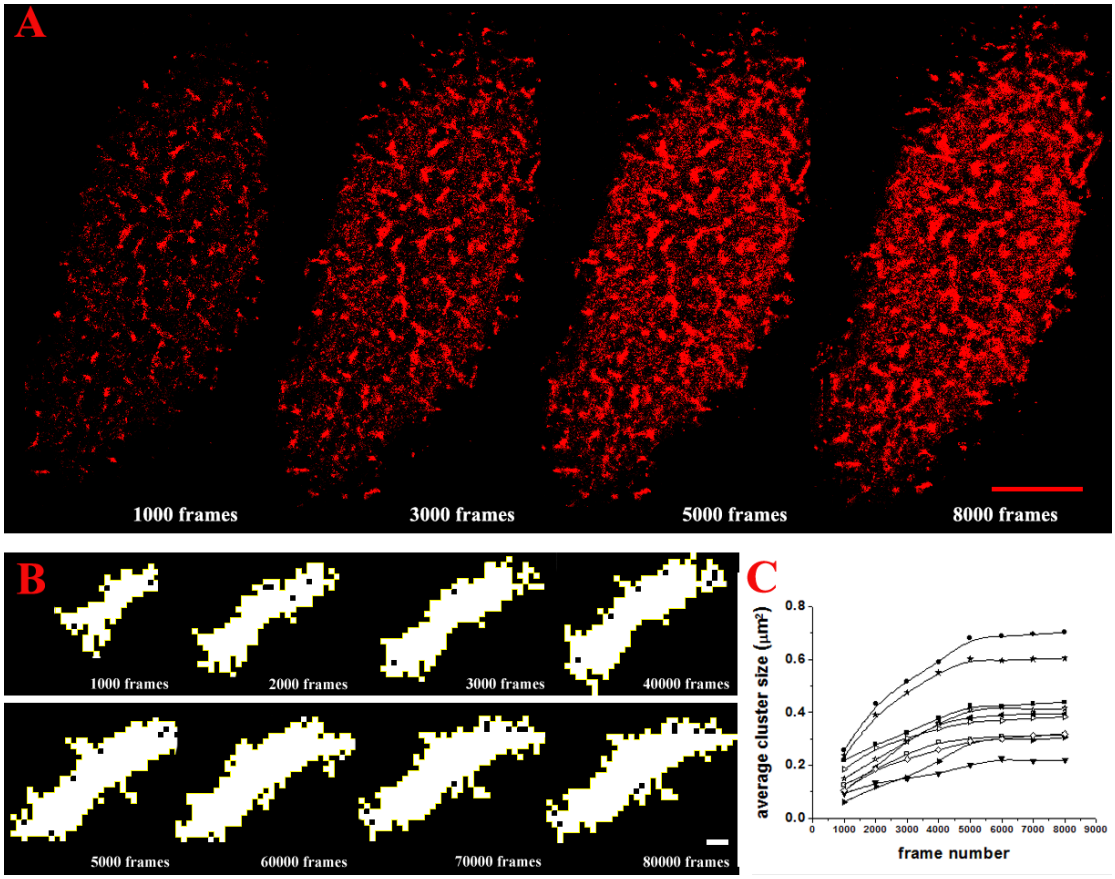

Figure S10. Statistical analyses of the trend in the distribution pattern of the N-GlcNAc with increasing the frame number. (A) the representative dSTORM images of the distribution of N-GlcNAcs were reconstructed from the increasing frame sequences. (B) the changes of the individual enlarged cluster with the increasing frame number. (C) the statistical analyses of the tread of the average cluster size with increasing frame number.

11. The improved resolution of dSTORM imaging was obviously achieved by comparing dSTORM image with TIRF image

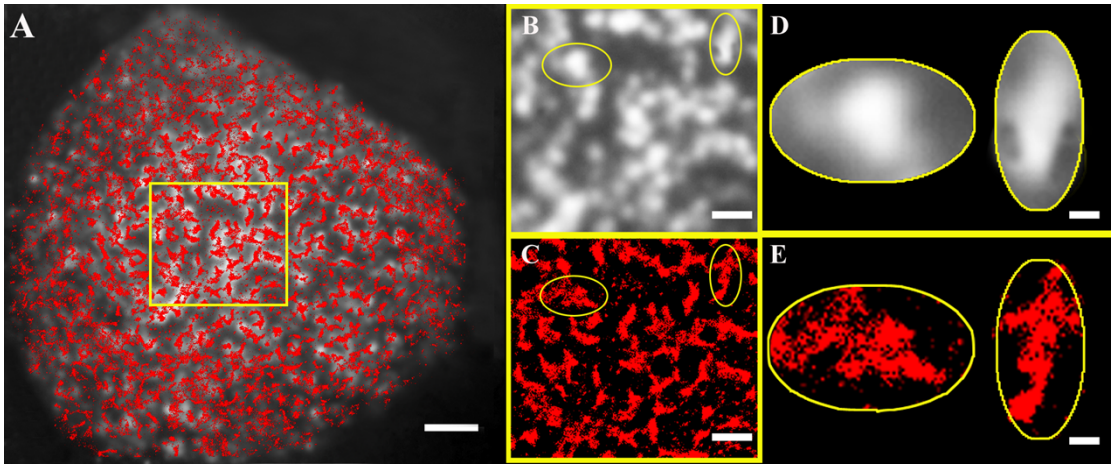

Figure S11. The comparison of the TIRF and dSTORM images of N-GlcNAcs on the Vero apical membrane. (A) The superimposed images of TIRF (gray) and corresponding dSTORM (red) from the entire apical membrane labeled with the Alexa647-WGA. (B and C) The enlarged images of TIRF and dSTORM from the box regions in Figure S11A. (D and E) The typical clusters from TIRF and dSTORM images show the dramatically improved resolution. Scale bars are 5 μm in A, 2 μm in B and C, 500 nm in D and E.

12. The dSTORM imaging has obvious advantage to profile the plasma membrane carbohydrates over other conventional imaging microscopies

In order to verify that dSTORM has advantage to image N-GlcNAcs on the cell membrane over other conventional imaging techniques, we also applied a high-resolution live cell imaging workstation (the Deltavision imaging system from Applied Precision which has comparable resolution with laser confocal fluorescence microscopy) to map N-GlcNAcs on the Vero basal membranes (Figure S12A-left). The resolution (blurry outline and no clear pattern) is much low compared with STORM image (Figure S12A-right). From the mask of the clusters abstracted from Deltacvision image (Figure S12B-left) and dSTORM image (Figure S12B-right), we found the clusters from Deltavision imaging were larger than those from dSTORM imaging, especially for the clusters on the membrane edge (Figure S12C). And this characterization was confirmed by comparing the average cluster size which was analyzed with the same method (Figure S12D). The results can demonstrate the dSTORM imaging has an improved resolution to characterized the molecular

distribution pattern with a clearer boundary in comparison with other conventional fluorescent imaging.

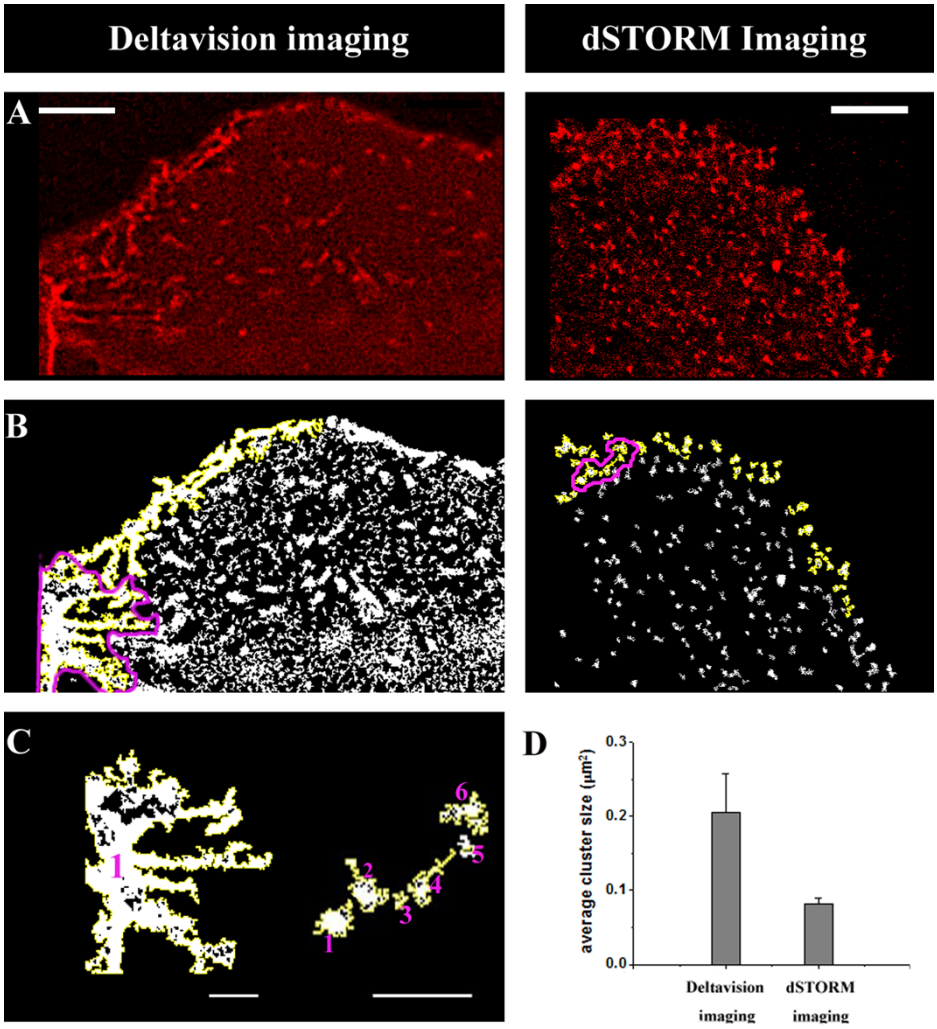

Figure S12. The images and cluster analyses of N-GlcNAcs on the Vero basal membranes from different imaging techniques. (A) The image of N-GlcNAcs by Deltavision imaging system (A-left) and dSTORM imaging (A-right). Scale bars are 5 μm. (B) the mask of clusters abstracted from Deltavision imaging system (A-left) and dSTORM imaging (A-right) with the same analysis method. (C) The enlarged clusters from Figure B with different levels in boundary segment. The big cluster as a whole (C-left) cannot be further segmented without clear boundary because of the low resolution of Deltavision imaging system. However, the small clusters (C-right) with clear boundary were abstracted from dSTORM image. Scale bars are 2 μm. (D) The statistical results of the average size of clusters inside the cell membrane abstracted from Deltavision imaging system and dSTROM imaging, with excluding the clusters which cannot be segmented on the membrane edge.

13. Semi-quantitative analyses of the average number of WGAs per cluster and the number of WGAs per unit area of the cell apical membrane.

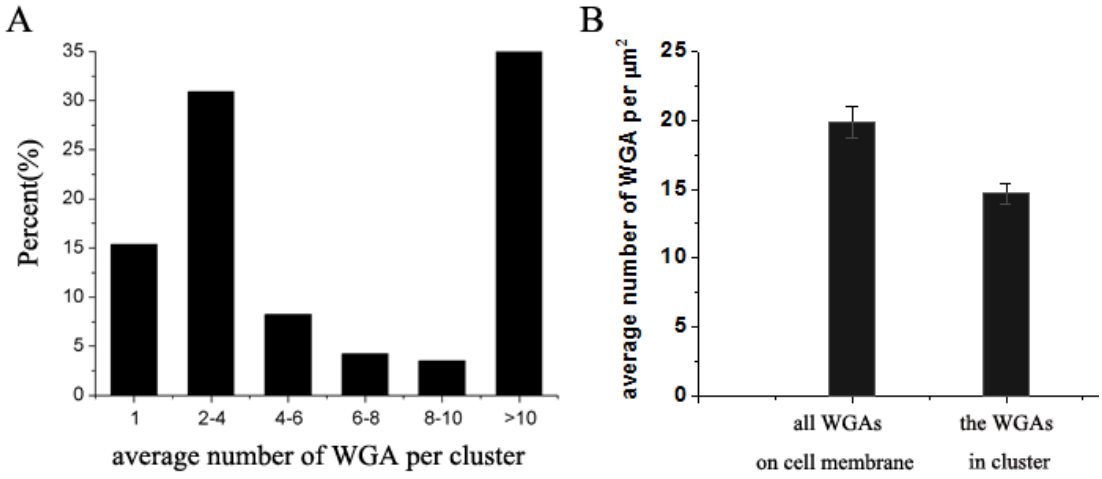

Figure S13. The semi-quantitative analyses of the binding WGA on the Vero apical membrane. (A) Histogram of the average number of WGAs per cluster. Data from 424 clusters on six cellular apical membranes, which were calculated via dividing the number of localizations per cluster by the average number of localizations from a single WGA. (B) the statistical results of the average number of the WGA on the cell membrane (left) and in cluster (right) per unit area of the cell apical membrane.

Experimental section for supporting information

Cleaning slides

To ensure that cover slides and microscope slides were quite clean, we treated them with the following procedures: firstly, twice ultrasonic cleaning in micro-90® concentrated cleaning solution (1:50 dilution with Milli-Q water, Sigma Aldrich), then rinsing with Milli-Q water to remove the pollutants; secondly, twice ultrasonic cleaning in Milli-Q water and twice ultrasonic cleaning in absolute ethyl alcohol, all ultrasonic cleaning were implemented with 15 min at low power; finally, the clean slides were kept in absolute ethyl alcohol. Prior to use, the slides were washed three times with sterile distilled water and dried with pure Argon.

The preparation of Alexa647-linked WGA

Wheat germ agglutinin (WGA), one of most widely used lectins[2] that have the carbohydrate recognition domain (CRD) to specifically combine with the sugar moieties of glycoproteins and glycolipids, is applied to recognize the N-GlcNAc in cellular membranes. Alexa Flour 647, as a favorable fluorescent probe, has been used in super-resolution imaging, because of its predominant properties in brightness, photostability and pH insensitivity.[3] Therefore, we used Alexa647-linkd WGA as fluorescent probe in our dSTORM imaging of N-GlcNAcs.

0.5 μL Alexa647 (Molecular Probes) were added to WGA solution (250 μL, 200 μg/mL), then reacted on rocking bed at 27°C for three hours with gentle vortex. Excrescent free Alexa647 were removed by a PD Spin Trap G-25 filtration column (GE Healthcare) with 1x PBS. The labeling ratio was calculated by measuring the absorbance of sample at 280 nm (WGA) and 650 nm (maximum absorbance of Alexa647). Then we obtained the ratio was ~ 0.5 to 1 Alexa647 per WGA by calculating with the Beer-Lambert law.

Determined the labeling concentration by plotting the concentration gradient curve

To make sure that all specific saccharide groups on Vero basal and apical membranes can be labeled and imaged, we determined the saturated concentration of Alexa647-conjugated WGA solution by plotting the curve of concentration gradient. From the curves, we found that the suitable experiment concentration was ~0.1 μM for the basal membrane and 0.08 μM for the apical membrane.

To determine the labeling concentration, we imported the lists of x, y coordinates gained from the results of QuickPALM analysis in ImageJ to Matlab. Then we used the custom program to plot the reconstruction image and calculated the number of localizations on cellular membrane with removing the localizations which are not belong to the imaged cells. For calculating the area of the cellular membrane, we exploited an intrinsic image process in ImageJ that can automatically find the outlines of cellular surface and compute the area of the interested cell. Certainly, when automatically finding was not able to effectively identify the interested cellular surface, we can also manually draw the outline of cells.

The imaging of N-GlcNAcs on the Vero basal membrane by the Applied Precision Deltavision imaging system

With the same culture conditions as those on the glass slide, the cells were cultured in the 35-mm glass bottom dish (Shengyou Biotechnology Co.,Ltd) for approximate 24 hours to achieve a ~70% confluence. After washing, fixing and labeling as those for the dSTORM imaging, the prepared sample maintained in 1 mL PBS (1X) was stored in 4°C before imaging. Then we used the Deltavision imaging system (Applied Precision) equipped with an Olympus IX71 inverted microscope to image N-GlcNAcs on the Vero basal membrane.

Semi-quantitative analyses of the average number of N-GlcNAcs per cluster

In the semi-quantitative analyses, we randomly selected a rectangle area (4-10 μm^2) in each cellular membrane to estimate the localization density in cluster via dividing the total number of localizations in the cluster by the average number of localizations per single WGA cluster (average 50 localizations per single WGA cluster, by analyzing 40 single WGA clusters from five independent experiments). For the density of WGA on the cell membrane, we calculated the localization density on cell membrane through diving the total number of localizations in the selected rectangle area by the area size of the rectangle area, then further estimated the density of the WGA on cell membrane via diving the localization density by the average number of localizations per single WGA cluster. Similarly, for the density of WGA in the cluster per unit area of the cell membrane, we calculated the localization density in the cluster, then, estimated the density of the WGA in the cluster.

References

(1) Afrough, B.; Dwek, M. V.; Greenwell, P. *BioTechniques* 2007, *43*, 458.

(2) Vijayan, M.; Chandra, N. *Curr. Opin. Struc. Biol.* 1999, *9*, 707.

(3) Dempsey, G. T.; Vaughan, J. C.; Chen, K. H.; Bates, M.; Zhuang, X. *Nat. Methods* 2011, *8*, 1027.